Lawrence Berkeley National Laboratory
LBL Publications

Title

Amphiphilic Heterografted Molecular Bottlebrushes with Tertiary Amine-Containing Side Chains as Efficient and Robust pH-Responsive Emulsifiers

Permalink

Journal

ISSN

Authors

Kelly, Michael T
Chen, Zhan
Russell, Thomas P
et al.

Publication Date

DOI

Copyright Information

Amphiphilic Heterografted Molecular Bottlebrushes with Tertiary Amine-Containing Side Chains as Efficient and Robust pH-Responsive Emulsifiers

Michael T. Kelly,[a] *Zhan Chen,*[b] *Thomas P. Russell,*[*,b,c] *and Bin Zhao*[*[a]]

[a]   M. T. Kelly, Prof B. Zhao
        Department of Chemistry
        University of Tennessee
        Knoxville, TN 37996 (USA)
        E-mail: bzhao@utk.edu

[b]   Z. Chen, Prof. T. P. Russell
        Department of Polymer Science and Engineering
        University of Massachusetts
        Amherst, MA 01003 (USA)
        E-mail: russell@mail.pse.umass.edu

[c]   Prof. T. P. Russell
        Materials Sciences Division, Lawrence Berkeley National Laboratory
        1 Cyclotron Road, Berkeley, CA 94720 (USA)

        Supporting information for this article is given via a link at the end of the document.

Abstract: By combining the unique characteristics of molecular bottlebrushes (MBBs) and the properties of stimuli-responsive polymers, we show that MBBs with randomly grafted poly(n-butyl acrylate) and pH-responsive poly(2-(N,N-diethylamino)ethyl methacrylate) (PDEAEMA) side chains are efficient and robust pH-responsive emulsifiers. Water-in-toluene emulsions were formed at pH 4.0 and disrupted by increasing the pH to 10.0. The emulsion generation and disruption was reversible over the ten cycles investigated, and the bottlebrushes remained intact. The exceptional emulsion stability stemmed from the high interfacial binding energy of MBBs, imparted by their large molecular size and Janus architecture at the interface, as evidenced by the interfacial jamming and wrinkling of the assemblies upon reducing the interfacial area. At pH 10.0, PDEAEMA became water-insoluble, and the MBBs desorbed from the interface, causing de-emulsification. Consequently, we have shown that the judicious design of MBBs can generate properties of particle emulsifiers from their large size, while the responsiveness of the MBBs enables more potential applications.

Introduction

Molecular bottlebrushes (MBBs) are a special class of graft copolymers featured by a polymer backbone with densely grafted polymeric side chains.[1] Due to the unique molecular structure, MBBs exhibit many intriguing characteristics and properties, such as minimal chain entanglement, high persistence length, stimuli-triggered conformational transitions, and unusual crystallization behavior.[1,2] There has been a growing interest in MBBs in recent years, from the development of new synthetic methods,[3] to the elucidation of their structures and self-assembly,[4] and the emergence of novel applications.[5] MBBs are commonly synthesized by three methods:[1,3] (i) grafting to, where end-functionalized polymers are covalently attached to a polymer backbone, (ii) grafting from, where side chains are grown from an initiator-functionalized polymer, and (iii) grafting through, where a macromonomer is polymerized directly into an MBB. Using click chemistry such as the copper(I)-catalyzed alkyne-azide cycloaddition (CuAAC) reaction, high grafting density MBBs can be routinely synthesized via the grafting-to method.[6]

Emulsions, where liquid droplets are dispersed in a second, immiscible liquid stabilized by a surfactant, are widely used in food, pharmaceutical, cosmetics, and oil industries.[7,8] MBBs can be applied as emulsion stabilizers.[8-15] Compared to small molecule and polymer surfactants, amphiphilic MBBs, with side chains composed of distinct hydrophilic and hydrophobic polymers, are structurally more versatile; their properties can be tailored by varying the lengths and types of backbone and side chain polymers, molar ratio of hydrophilic to hydrophobic side chains, and grafting density.[8] Upon adsorption to the water-oil interface, amphiphilic bottlebrushes can spontaneously re-configure into a hydrophilic-rich and hydrophobic-rich conformation, i.e., a Janus architecture, where the hydrophilic side chains extend into the aqueous phase and the hydrophobic side chains reside in the organic phase.[9a,10a,13,15] The distinct affinities of two side chain

polymers for different liquid phases result in a strong interfacial binding of the MBBs. Consequently, MBBs, if judiciously designed, could be irreversibly adsorbed to the interface, although this has not been demonstrated. This is in stark contrast to the fast adsorption and desorption dynamics at the interface exhibited by low molar mass and typical polymeric surfactants.[16] The large molecular size and the interfacial Janus structure of MBBs result in a high energy requirement to remove the brushes from the interface, affording high emulsion stability. In this regard, MBBs can behave similarly to Janus particles used for Pickering emulsions,[17-19] where sufficiently large particles are irreversibly trapped at the interface. Note that for the MBBs reported as emulsifiers, one of side chain polymers is soluble in both liquids, and thus the brush configuration at the interface may be better described as a hydrophilic- and hydrophobic-rich architecture, which may not be ideal for stabilizing emulsions. The strong adsorption of MBBs to the interface and the resultant high stability of emulsions have been reported.[9,10,13] By exploiting the electrostatic interactions between water-soluble poly(acrylic acid) MBBs and toluene-soluble amine-functionalized polyhedral oligomeric silsesquioxane at the water-toluene interface, the formation of various types of emulsions and the interfacial jamming of molecular assemblies were demonstrated.[20] In addition, amphiphilic MBBs have been reported to exhibit a decreased tendency to form intermolecular self-assemblies in bulk liquid phases compared to analogous diblock copolymers.[9a,10a] Thus, stable emulsions can be achieved at lower concentrations with MBBs, meaning a higher emulsification efficiency, although MBBs do not necessarily favor the generation of smaller emulsion droplets.[10a] Moreover, the densely grafted brush architecture can reduce the thinning of films during coalescence, further enhancing the stability of emulsions.

For many applications such as crude oil recovery, it is highly desired to use stimuli-responsive emulsions that are very stable under certain conditions but readily disrupted by an external stimulus, such as a pH or temperature change.[21-26] Such systems could significantly enhance separation efficiencies and reduce energy consumption.[27] There are many examples of stimuli-responsive emulsions,[21-26] but few using MBBs. Herein, we report the design and synthesis of MBBs with heterografted poly(n-butyl acrylate) (PnBA) and pH-responsive poly(2-(N,N-diethylamino)ethyl methacrylate) (PDEAEMA) side chains (Figure 1A,B) and the investigation of their utility as stimuli-responsive emulsifiers. The pK_a of protonated PDEAEMA is 7.4, above which PDEAEMA is insoluble in water.[28,29] Thus, at an acidic pH, PDEAEMA is protonated and only soluble in water, while PnBA is only soluble in an organic phase, which would generate a Janus structure at the interface for stabilizing emulsions. When the pH is increased above the pK_a, PDEAEMA becomes water-insoluble; the

reduced amphiphilicity would cause MBBs to desorb from the interface and the disruption of emulsions. A click grafting-to approach was used to prepare MBBs (Figure 1A,B).[6] This method allows for a facile tuning of the side chain composition while maintaining the backbone and side chain lengths, enabling a better understanding of how side chain composition affects MBBs' abilities to act as emulsifiers. The emulsification and interfacial behaviors of these MBBs were investigated, and we show that MBBs with appropriate side chain compositions are efficient and robust pH-responsive emulsifiers, exhibiting the desired properties of both particle surfactants and stimuli-responsive polymers.

Results and Discussion

Synthesis and Characterization of MBBs

Four heterografted and two homografted brush polymers were prepared using the CuAAC reaction to graft alkyne-end-functionalized PnBA and/or PDEAEMA onto an azide-bearing polymer backbone (PHEMA-N$_3$, Figure 1A,B). PHEMA-N$_3$, with a degree of polymerization (DP) of 406, a dispersity ($Đ$) of 1.12, and an azide functionalization of 97.5%, was synthesized by atom transfer radical polymerization (ATRP) of 2-((trimethylsilyl)oxy)ethyl methacrylate and post-polymerization reactions to install azide groups. Alkyne-end-functionalized side chain polymers, PnBA and PDEAEMA, with DPs of 51 and 44, respectively, were prepared by ATRP of the respective monomers using propargyl 2-bromoisobutyrate as the initiator. Size exclusion chromatography (SEC) analysis of these polymers showed low dispersities ($Đ$ ≤ 1.10). Heterografted MBBs were synthesized using different feed molar ratios of PnBA and PDEAEMA and an excess of side chain polymers relative to the backbone repeat units, ~ 1.3 – 1.4 : 1, to obtain high grafting densities. Homografted PnBA and PDEAEMA MBBs were prepared using similar conditions. The unreacted side chain polymers were removed, which was verified by SEC. The molar ratios of PnBA and PDEAEMA in the MBBs were found to be similar to the initial feed ratios. The grafting densities of these MBBs, determined from SEC or ^{1}H NMR analysis, were high, in the range of 86.7% – 94.5%. The synthesis of precursor polymers and MBBs can be found in the Supporting Information (SI), and the characterization data are summarized in Tables S1 and S2. We denote these polymers as MBB-B$_x$E$_y$, where B and E represent PnBA and PDEAEMA, and x and y correspond to the mole fractions of PnBA and PDEAEMA side chains, respectively. Figure 1C-H shows atomic force microscopy (AFM) images of six MBBs, exhibiting a wormlike morphology with relatively uniform lengths. Analysis indicated that the average lengths of MBBs were very similar, ~ 100 nm, except MBB-B$_{0.00}$E$_{1.00}$, which was 109.2 ± 26.5 nm, likely caused by different AFM sample preparation conditions (see Figure 1 caption).

The very similar molecular lengths and length distributions of the six MBBs were derived from the same backbone and side chain polymers and comparable grafting densities, allowing for a better understanding of the effect of side chain composition on emulsification behavior.

MBBs as pH-Responsive Emulsion Stabilizers: Effect of Side Chain Composition

We first investigated the abilities of four heterografted MBBs to function as emulsifiers for a mixture of toluene and a 1.0 mM aqueous phosphate buffer with pH 4.0, at which PDEAEMA was fully protonated. The 1.0 mM buffer was used to minimize the long-range electrostatic interactions and help ensure accurate pH measurements. Three concentrations of MBBs, 0.02, 0.01, and 0.005 wt%, were examined relative to the total mass of toluene and the buffer. Because the addition of a tertiary-amine-containing MBB into the mixture will change the pH of the aqueous phase and there is a difficulty in measuring the pH after emulsion formation, an indirect method is adopted to obtain
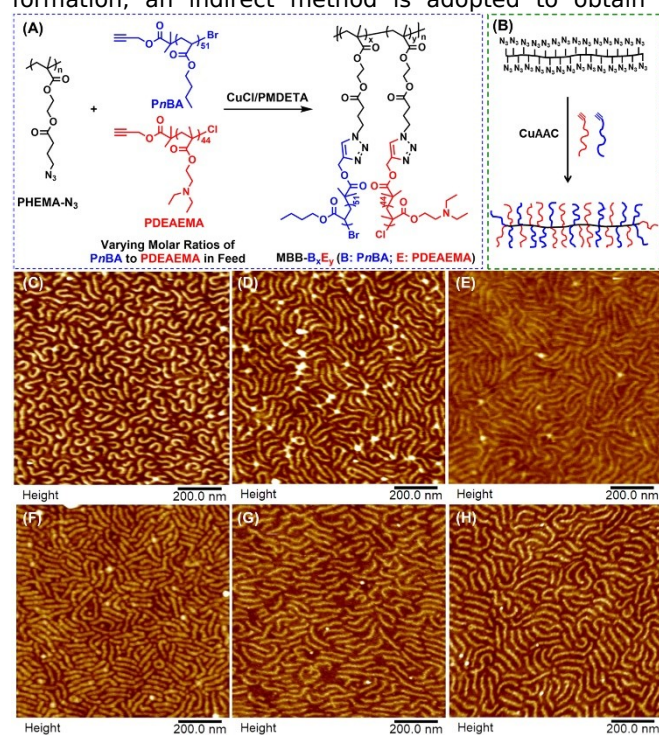
Figure 1. Synthesis of MBB-B_xE_y MBBs using a click grafting-to method (A) and schematic illustration (B). AFM images of (C) MBB-$B_{1.00}E_{0.00}$ (average contour length of 251 bottlebrushes: 100.1 ± 23.6 nm, sample prepared using a Langmuir-Blodgett (LB) trough on Milli-Q water), (D) MBB-$B_{0.80}E_{0.20}$ (average length of 250 molecules: 100.6 ± 28.2 nm), (E) MBB-$B_{0.64}E_{0.36}$ (average length of 217 brushes: 102.4 ± 26.4 nm), (F) MBB-$B_{0.51}E_{0.49}$ (average length of 287 bottlebrushes: 99.8 ± 26.9 nm), (G) MBB-$B_{0.24}E_{0.76}$ (average length of 234 bottlebrushes: 99.2 ± 30.2 nm), (H) MBB-$B_{0.00}E_{1.00}$ (average length of 211 molecules: 109.2 ± 26.5 nm, sample prepared on a pH 10.0 aqueous subphase using LB). The AFM samples for (D)-(G) were prepared using an LB trough with a pH 4.0 aqueous subphase.

desired pH values detailed below. For each concentration of an MBB in the mixture of toluene and the aqueous solution, we calculated the mass of PDEAEMA from the characterization data of MBBs and assumed that tertiary-amine-containing side chains can be fully exposed to the aqueous phase. To determine the amount of a HCl or a NaOH solution needed to bring the pH to a desired value, an aqueous solution of the alkyne-end-functionalized PDEAEMA with the same concentration as in the aqueous phase of PDEAEMA side chains of the MBB in the emulsion mixture was prepared using the 1.0 mM buffer with pH 4.0. The pH of the PDEAEMA solution was adjusted back to 4.0 by gradually adding a 1.0 or 0.1 M HCl solution, then to pH = 10.0 using a 1.0 or 0.1 M NaOH solution, and back to pH 4.0. The same amounts of HCl and NaOH were applied to the mixture of toluene containing the MBB and the 1.0 mM buffer with an initial pH of 4.0 to achieve desired pH of 4.0 and 10.0.

Each mixture of toluene, containing an MBB, and the 1.0 mM solution, with a presumed pH of 4.0 after PDEAEMA side chains were fully exposed to the aqueous phase, was vortexed for 60 sec, divided into two intervals with 5-10 min in between. Emulsions were formed with MBB-$B_{0.80}E_{0.20}$, MBB-$B_{0.64}E_{0.36}$, and MBB-$B_{0.51}E_{0.49}$ as stabilizers (Figure 2), and even with the use of only 0.005 wt% of MBBs, the emulsions were stable over a long period of time. For MBB-$B_{0.24}E_{0.76}$, emulsions were formed initially; however, they were unstable and disrupted after a few hours. We also tested MBB-$B_{1.00}E_{0.00}$ and MBB-$B_{0.00}E_{1.00}$ under the same conditions, and no stable emulsions formed. The emulsions generated with MBB-$B_{0.80}E_{0.20}$, MBB-$B_{0.64}E_{0.36}$, and MBB-$B_{0.51}E_{0.49}$ were water-in-oil emulsions, determined by adding the emulsion droplets into toluene and water as the droplets were dispersed in toluene but not in water.[10a] This was further supported by laser confocal microscopy using Nile Red, which is soluble in toluene but not in water, as a fluorescent probe. As shown in Figure 2G,H, the continuous phase was red, while the dispersed phase was dark, indicating that the continuous phase was toluene. To study if there were differences in the abilities of MBB-$B_{0.80}E_{0.20}$, MBB-$B_{0.64}E_{0.36}$, and MBB-$B_{0.51}E_{0.49}$ in stabilizing emulsions, we used an optical microscope to examine the emulsion droplets for all three concentrations. Although the droplet sizes and distributions were similar at 0.02 wt% for three MBBs, the droplets in the samples with 0.01% and 0.005% MBB-$B_{0.80}E_{0.20}$ appeared to be larger than those stabilized by the other two MBBs at the same concentrations (Figure S20 in the SI). The differences between the emulsions with MBB-$B_{0.64}E_{0.36}$ and MBB-$B_{0.51}E_{0.49}$ were subtler; however, MBB-$B_{0.51}E_{0.49}$ appeared to perform the best, likely a result of its more symmetric side chain composition. We note here that it is possible that some bottlebrushes were left in the toluene phase after the interface was fully covered by other brush molecules. The relatively large size distribution of emulsion droplets was presumably caused by the

essentially irreversible adsorption of the bottlebrushes to the interface as discussed later. Consequently, the system was likely locked in a nonequilibrium state. Based on the observation of emulsification behaviors of six MBBs, there is a side chain composition range for MBBs to act as effective emulsifiers (Figure 2I). Interestingly, this composition range is not symmetric, possibly because protonated PDEAEMA at pH 4.0 exhibits a stronger affinity toward water than PnBA toward toluene, resulting in an intrinsic curvature of bottlebrushes significantly different from that of the water-toluene interface during emulsification. However, many factors are known to affect the formation of emulsions.[8,21]

To investigate the pH-responsive behavior of the emulsions stabilized by those three MBBs, for each mixture, a NaOH solution was introduced to change the pH from 4.0 to 10.0, at which PDEAEMA was nearly fully deprotonated. Shortly after the addition of NaOH, we observed that the emulsion droplets began to coalesce and eventually the emulsions were broken (Figure 2B,C,D). With gentle stirring by a stirbar at 60 rpm, the breaking
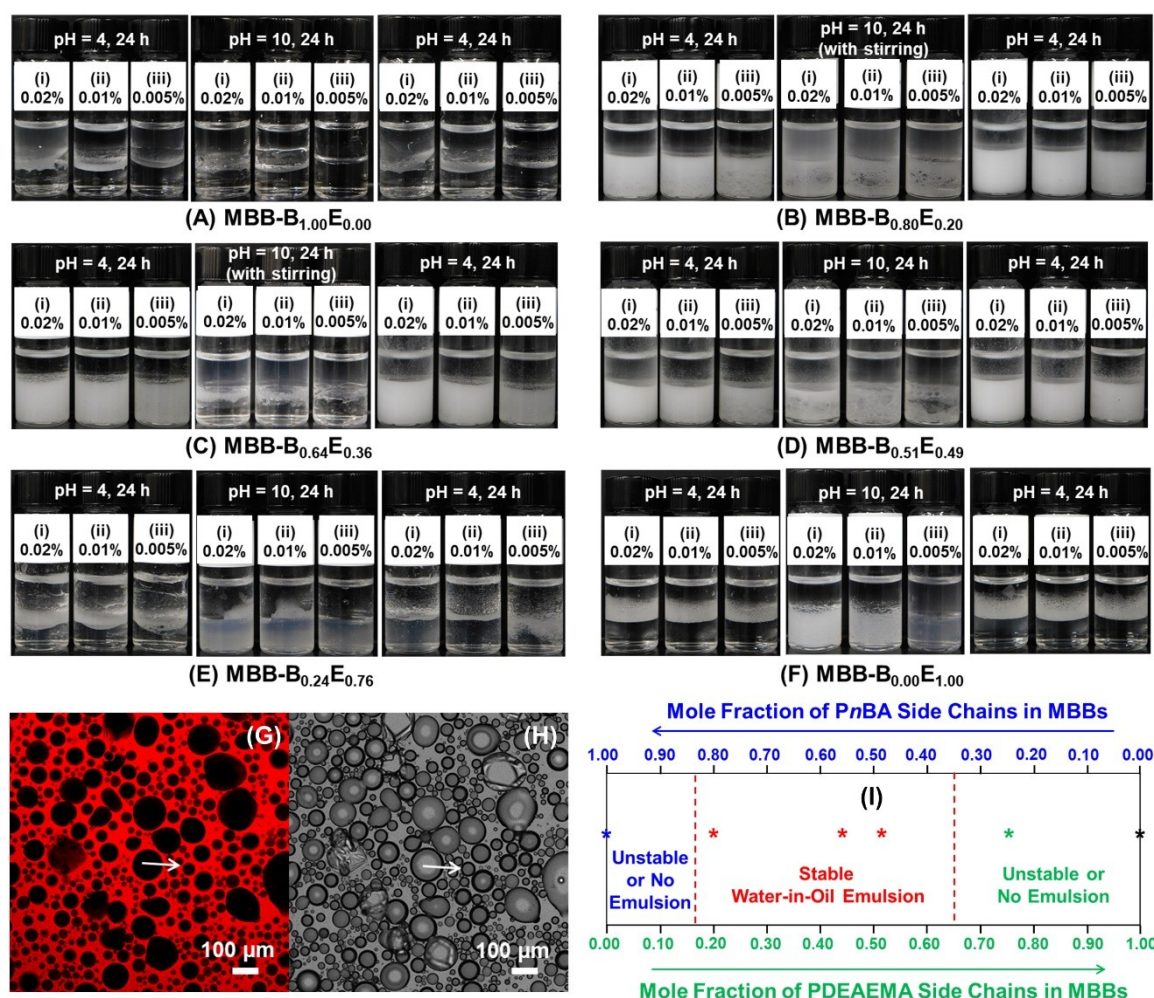
Figure 2. Optical photos of the mixtures of toluene with an MBB and a 1.0 mM buffer at pH 4.0 after vortexing for 60 sec and sitting still for 24 h, at pH 10.0 after NaOH addition and gentle shaking for 30 sec, and at pH 4.0 after HCl addition and vortexing for 60 sec again for MBB-B$_{1.00}$E$_{0.00}$ (A), MBB-B$_{0.80}$E$_{0.20}$ (B), MBB-B$_{0.64}$E$_{0.36}$ (C), MBB-B$_{0.51}$E$_{0.49}$ (D), MBB-B$_{0.24}$E$_{0.76}$ (E), and MBB-B$_{0.00}$E$_{1.00}$ (F) at concentrations of 0.02 wt% (i), 0.01 wt% (ii), and 0.005 wt% (iii). For MBB-B$_{0.80}$E$_{0.20}$ and MBB-B$_{0.64}$E$_{0.36}$, the mixtures at pH 10.0 were stirred with a stirbar at 60 rpm for a few hours to facilitate the emulsion breaking. Laser confocal image (G) and optical micrograph (H) of the emulsion with 0.02 wt% MBB-B$_{0.51}$E$_{0.49}$ at pH 4.0. Nile Red was added as a fluorescent dye. The marked droplet in Figure 2G,H was 50 μm in diameter. (I) Side chain composition range of MBBs for functioning as effective emulsifiers at pH 4.0.

of emulsions was slightly faster. For the samples that did not form emulsions at pH 4.0, we vortexed them under the basic condition for 60 sec. No emulsions were produced for MBB-B$_{1.00}$E$_{0.00}$ as expected (Figure 2A). For MBB-B$_{0.24}$E$_{0.76}$, the bottom layers were cloudy solutions after 24 h (Figure 2E). Interestingly, MBB-B$_{0.00}$E$_{1.00}$

formed an emulsion layer with rather large droplets, visible to the naked eye, after vortexing at concentrations of ≥ 0.01 wt%. With gentle stirring for ~ 2 h by a stirbar, the bottom layer of the 0.01 wt% sample became a mainly cloudy solution, though some large droplets were still visible at the bottom of the vial. It was believed that the 0.02 wt% sample would need a longer time for the droplets to coalesce.

The pH for all samples was then adjusted back to 4.0 by adding a HCl solution, and the vials were gently shaken to allow HCl to diffuse into the aqueous phase. The vials were then vortexed for 60 sec as in the first time, and water-in-oil emulsions were re-generated for MBB-$B_{0.80}E_{0.20}$, MBB-$B_{0.64}E_{0.36}$, and MBB-$B_{0.51}E_{0.49}$. There were no noticeable differences between the first and the second vortexing after 24 h for the same MBB at the same concentration. Similar to the first round of vortexing, no stable emulsions were observed for the other three MBBs.

Stability of MBB-$B_{0.51}E_{0.49}$-Stabilized Emulsions

To study the emulsion stability, we prepared two emulsions at pH 4.0 using 0.02 and 0.01 wt% MBB-$B_{0.51}E_{0.49}$. The vials were stored in a desiccator saturated with water and toluene vapors (achieved with open vials of water and toluene). The macroscopic appearance and the emulsion droplets were examined by eye and optical microscopy, respectively, at different times over a period of 6 weeks, and the results are shown in Figure 3. There were no discernable changes in the optical micrographs of emulsion droplets, demonstrating the high stability of both emulsions. Note that the changes of the heights of the top clear layer and the bottom emulsion layer for both emulsions were likely caused by multiple rounds of the removal of a portion of the sample for optical microscopy study of emulsion droplets.
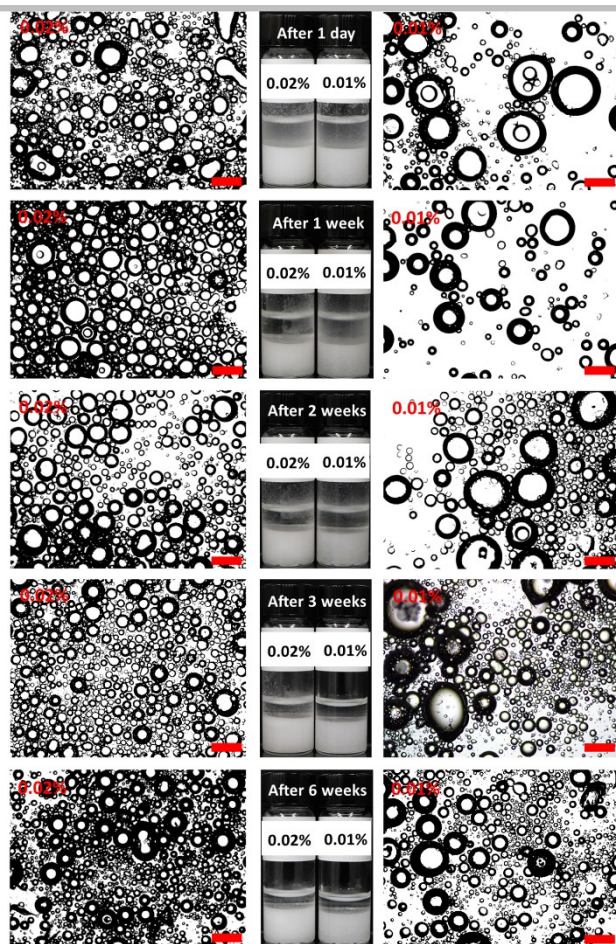
Figure 3. Optical micrograph of emulsion droplets from the 0.02 wt % emulsion (left), photo of two emulsions (middle), and optical micrograph of emulsion droplets from the 0.01 wt% emulsion (right) with MBB- $B_{0.51}E_{0.49}$ as stabilizer at pH 4.0 after 1 day (top row), one week (2nd row), two weeks (3rd row), three weeks (4th row), and six weeks (5th row). Scale bars: 200 μm.

Repeatability of pH-Induced Formation and Breaking of Emulsions

From a practical point of view, it would be advantageous if the emulsions could be reversibly formed for multiple cycles. MBB-$B_{0.51}E_{0.49}$ was selected to investigate the repeatability of emulsion formation and disruption at four concentrations, 0.03, 0.02, 0.01, and 0.005 wt%. Once the emulsions were generated at pH 4.0, they were left for ≥ 6 h prior to imaging and recording optical micrographs. Subsequently, a NaOH solution was added to the mixture to change the pH to 10.0 along with a stirbar to facilitate the breaking of emulsions. After the addition of HCl to decrease the pH back to 4.0, the emulsions were re-generated by vortexing.

A total of 10 cycles were performed, and we found that for the three higher concentrations (0.03, 0.02, and 0.01%), the mixtures were able to go through 10 full emulsion formation and breaking cycles (Figure 4A). For
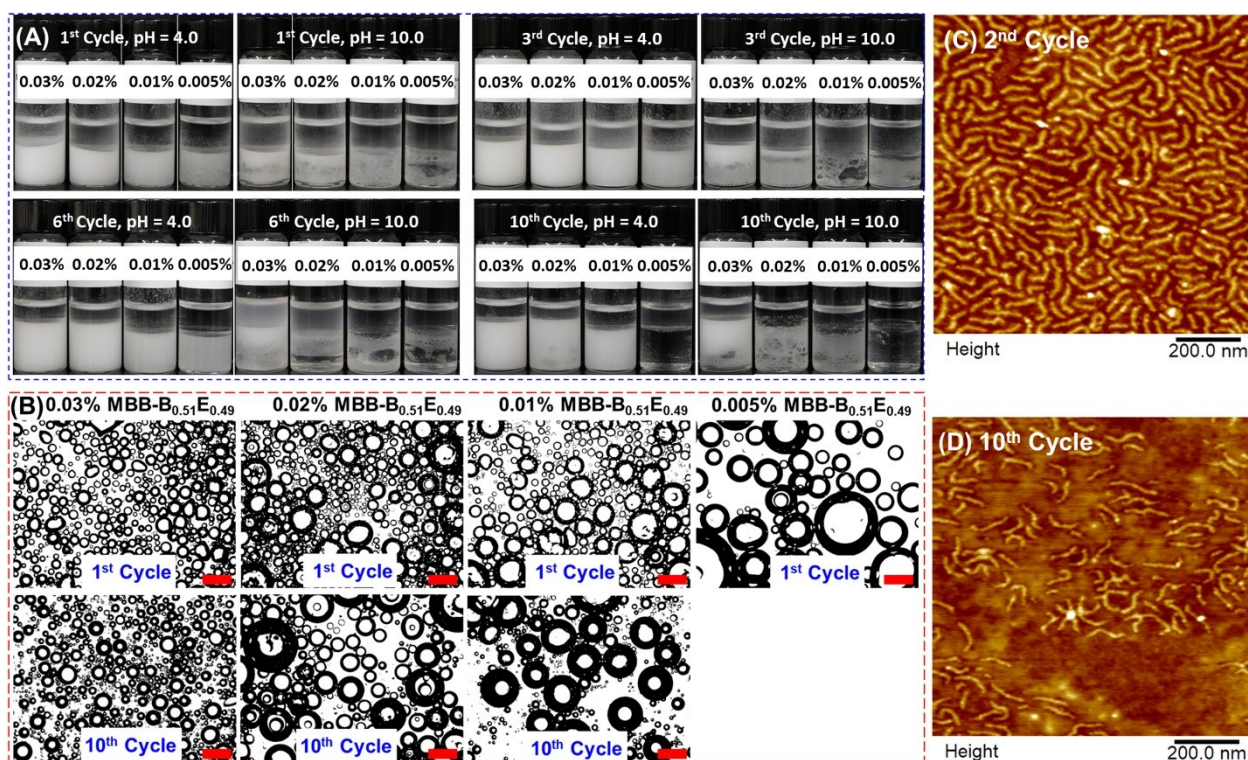
5

the mixture with a 0.005 wt% concentration, an emulsion was formed under acidic conditions in the first eight cycles but not in the last two cycles. Despite the visual observation of emulsion formation for the three higher concentrations over ten cycles, optical micrographs from the first and tenth cycles showed that the emulsion droplets were slightly larger after the tenth cycle for concentrations of 0.02 and 0.01 wt%, while for the 0.03 wt% mixture the droplet sizes were similar (Figure 4B). This observation and the absence of emulsion formation for the 0.005 wt% mixture in the last two cycles were likely caused by the accumulation of the salt in the aqueous phase after the introduction of HCl and NaOH, which reduced the emulsion stability. We noticed that the emulsion layer gradually became taller with successive formation-breaking cycles. This is likely a result of the increased volume of the aqueous phase after multiple rounds of addition of HCl and NaOH solutions – a total of ~ 200 µL of aqueous solutions was injected after 10 cycles.

To determine if there were any changes to the MBB after the repeated emulsion formation and breaking, a small portion of the emulsion layer was withdrawn from the vial in the 2nd and 10th cycle and deposited onto the surface of a 1.0 mM aqueous phosphate subphase in an LB trough for preparing AFM samples. Figure 4C,D shows the AFM images of wormlike bottlebrushes. The average length of bottlebrushes was 98.2 ± 25.5 nm from the 2nd cycle (230 brushes measured) and 100.8 ± 28.2 nm from the 10th cycle (102 brushes measured), essentially the same as that of the original MBB (99.8 ± 26.9 nm, 287 bottlebrushes, Figure 1F). Given the very close values of the average brush length, this demonstrated that the MBB remained intact.

Interfacial Tension Reduction by MBBs and Interfacial Jamming of MBBs

The adsorption of MBBs at the acidic water-toluene interface for stabilization of emulsions and the desorption at pH 10.0 would cause changes in interfacial tension (γ). To better understand the interfacial behavior of MBBs and the mechanism for the stabilization of emulsions by those three MBBs, we conducted two pendant drop experiments: (i) measuring the time-dependence of γ by pendant drop tensiometry[15] and (ii) reducing the droplet volume and hence, interfacial area by withdrawing the droplet to determine how strongly MBBs were adsorbed to the interface at pH 4.0 and 10.0. A toluene droplet containing a 0.2 mg/g MBB with a volume of 7 µL was injected into a 10 mL aqueous solution with pH of 4.0 or 10.0, and γ was monitored as a function of time. For the pure water-toluene interface, γ is 35 mN/m.[15a] The time-dependences of γ for six MBBs at the two pH values are shown in Figure 5A,B. As expected, MBB-B$_{1.00}$E$_{0.00}$ showed minimal reduction in γ at both pH 4.0 and 10.0. In contrast, other MBBs displayed larger reductions in γ at both pH values, where an initial rapid decrease in γ was followed by a period of a gradual change (Figure 5A,B). At pH 4.0, the initial decrease in γ was greater with increasing mole fraction of PDEAEMA ($x_{PDEAEMA}$) in the side chains. For MBB-B$_{0.00}$E$_{1.00}$ and MBB-B$_{0.24}$E$_{0.76}$, γ showed large drops to ~ 15 mN/m within 20 s, while in that same time frame γ only decreased to ~ 26 mN/m for MBB-B$_{0.80}$E$_{0.20}$. The initial rapid

(A) 1st Cycle, pH = 4.0 | 1st Cycle, pH = 10.0 | 3rd Cycle, pH = 4.0 | 3rd Cycle, pH = 10.0
0.03% 0.02% 0.01% 0.005%
6th Cycle, pH = 4.0 | 6th Cycle, pH = 10.0 | 10th Cycle, pH = 4.0 | 10th Cycle, pH = 10.0

(B) 0.03% MBB-B$_{0.51}$E$_{0.49}$ | 0.02% MBB-B$_{0.51}$E$_{0.49}$ | 0.01% MBB-B$_{0.51}$E$_{0.49}$ | 0.005% MBB-B$_{0.51}$E$_{0.49}$
1st Cycle
10th Cycle

(C) 2nd Cycle
Height   200.0 nm

(D) 10th Cycle
Height   200.0 nm

Figure 4. Optical photos (A) of mixtures of toluene, a 1.0 mM buffer, and MBB-$B_{0.51}E_{0.49}$ at concentrations of 0.03, 0.02, 0.01, and 0.005 wt% for the formation and breaking of emulsions from the 1st, 3rd, 6th, and 10th cycle. (B) Optical micrographs of emulsion droplets from the 1st and 10th cycle at different brush concentrations. Scale bars: 200 μm. AFM images of MBB-$B_{0.51}E_{0.49}$ from the emulsions in the 2nd (C) and 10th cycle (D). AFM samples were prepared using an LB trough.

decrease is characteristic of the adsorption of bottlebrushes to the interface and conformational re-configurations.[15a] After the first stage, MBB-$B_{0.00}E_{1.00}$ rapidly reached a quasi-equilibrium γ (γ_{qe}) at ~ 9.5 mN/m. Such a large reduction in γ by MBB-$B_{0.00}E_{1.00}$ was unexpected, since protonated MBB-$B_{0.00}E_{1.00}$ is soluble in water. In fact, γ showed a very slight increase with time after the initial drop, suggesting a transient state of MBB-$B_{0.00}E_{1.00}$ where the adsorption to the interface was followed by a transfer from toluene to the aqueous phase.

Figure 5A also shows that the four heterografted MBBs behaved very differently after the initial rapid decrease. For MBB-$B_{0.80}E_{0.20}$, γ leveled off rapidly at γ_{qe} of ~ 21 mN/m. The other three heterografted MBBs never reached a quasi-equilibrium; rather, γ continued to decrease to ~ 5 mN/m, whereupon the pendant drop fell off the needle tip. The rate of decrease in the second stage increased with increasing $x_{PDEAEMA}$ in the side chains. This 2nd stage reflects a reorganization of the MBBs at the interface to achieve better packing.[15a] The lowest value of γ (γ_l) observed decreased with increasing $x_{PDEAEMA}$, from 21.0 mN/m for MBB-$B_{0.80}E_{0.20}$, to 5.0 mN/m for MBB-$B_{0.64}E_{0.36}$, 4.9 mN/m for MBB-$B_{0.51}E_{0.49}$, and 2.9 mN/m for MBB-$B_{0.24}E_{0.76}$. Note that despite the large reductions in γ for MBB-$B_{0.24}E_{0.76}$ and MBB-$B_{0.00}E_{1.00}$, emulsions could not be formed at pH 4.0. However, MBB-$B_{0.80}E_{0.20}$ that reduced γ to 21.0 mN/m could produce emulsions. At pH 10.0, the time-dependence of γ for MBB-$B_{0.80}E_{0.20}$ was similar to that at pH 4.0, and γ_{qe} was 22.5 mN/m (Figure 5B), only slightly higher than that at pH 4.0. For the other three heterografted MBBs and MBB-$B_{0.00}E_{1.00}$, γ decreased very slowly after the initial rapid drop. These four MBBs reduced γ to similar values, ~ 12.8 to 14.1 mN/m.

Considering the γ for pure water and toluene, the interfacial tension reductions observed here were quite large; however, emulsions were not formed for all at pH 10.0.

While the differences in γ_{qe} between pH 4.0 and 10.0 for MBB-$B_{1.00}E_{0.00}$ and MBB-$B_{0.80}E_{0.20}$ were quite small (< 2 mN/m), the changes for MBB-$B_{0.64}E_{0.36}$, MBB-$B_{0.51}E_{0.49}$, and MBB-$B_{0.24}E_{0.76}$ were large (~ 8 – 10 mN/m). On the other hand, the γ_l increased by ~ 4 mN/m for MBB-$B_{0.00}E_{1.00}$. Recall that only MBB-$B_{0.80}E_{0.20}$, MBB-$B_{0.64}E_{0.36}$, and MBB-$B_{0.51}E_{0.49}$ can act as pH-responsive emulsifiers. At pH 4.0, they produced emulsions that were broken when the pH was increased to pH 10.0. The small difference in γ_{qe} between the two pH values for MBB-$B_{0.80}E_{0.20}$ is puzzling, but may be attributed to the short measurement time (~ 20 min), while the breaking of emulsions occurred over longer times. These data show that a reduction in γ is necessary but not sufficient for the stabilization of emulsions, and the emulsion disruption is associated with an increase in γ.

We further investigated the interfacial binding of MBBs by the withdrawing of pendant drops containing a 0.2 mg/g MBB to reduce the volume and hence, interfacial area to see if the bottlebrushes were jammed at the interface. This experiment is analogous to lateral compression of MBBs at the interface. As mentioned earlier, for heterografted MBBs with $x_{PDEAEMA} \geq 0.36$ at pH 4.0, the toluene drop spontaneously pinched off when γ decreased to low values. Therefore, for these polymers, the volume reduction experiment was performed at the onset of the slow change stage for γ. Figure 5C,D shows the optical images of
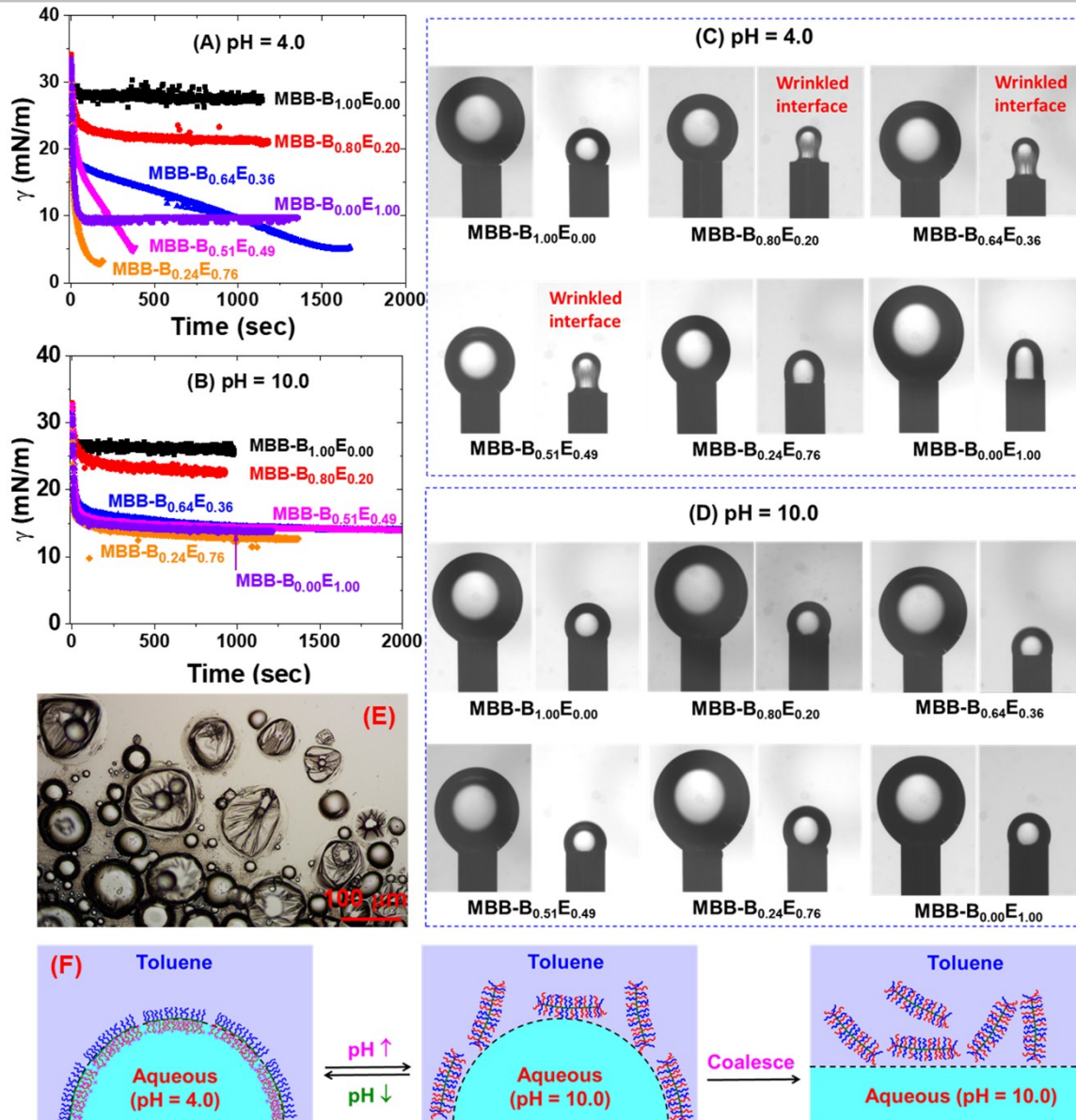
Figure 5. Time dependences of γ between toluene, containing a 0.2 mg/g MBB, and an aqueous solution with pH 4.0 (A) and 10.0 (B) measured by pendant drop tensiometry for six MBBs. (C) Photos of a toluene droplet containing 0.2 mg/g MBBs injected into a pH 4.0 aqueous solution and then withdrawn for MBB-$B_{1.00}E_{0.00}$, MBB-$B_{0.80}E_{0.20}$ at γ = 23 mN/m, MBB-$B_{0.64}E_{0.36}$ at γ = 20 mN/m, MBB-$B_{0.51}E_{0.49}$ at γ = 18 mN/m, MBB-$B_{0.24}E_{0.76}$ at γ = 15 mN/m, and MBB-$B_{0.00}E_{1.00}$ at γ = 10 mN/m. (D) Photos of a toluene droplet containing 0.2 mg/g MBBs injected into a pH 10.0 solution and then withdrawn. For each sample in (C) and (D), the left shows the initial state and the right shows the droplet before being fully withdrawn into the syringe. (E) Optical micrograph of partially dried emulsion droplets from a 0.03 wt% MBB-$B_{0.51}E_{0.49}$-stabilized emulsion at pH 4.0. (F) Schematic illustration of emulsion formation and disruption with MBBs as pH-responsive emulsifier.

toluene drops in the initiate state and at the point where they were about to be withdrawn into the syringe, obtained from the videos in the SI (Video-1 to -6 for pH 4.0 and Video-7 to -12 for pH 10.0). At pH 4.0, only MBB-$B_{0.80}E_{0.20}$, MBB-$B_{0.64}E_{0.36}$, and MBB-$B_{0.51}E_{0.49}$ showed interfacial wrinkling, evidencing that these bottlebrushes were strongly adsorbed to the interface. This is the first experimental observation that MBBs alone were jammed at the interface, producing wrinkled interfaces. Although a large reduction in γ was found for MBB-$B_{0.24}E_{0.76}$ and MBB-$B_{0.00}E_{1.00}$ at pH 4.0, no jamming was observed, indicating that their interfacial binding

energies were low, likely because MBB-$B_{0.00}E_{1.00}$ is soluble in acidic water and MBB-$B_{0.24}E_{0.76}$ might desorb into water as unimolecular micelles. At pH 10.0, no wrinkling behavior was observed, despite the significant reductions in γ for PDEAEMA-containing MBBs. These observations correlated well with the emulsification behaviors of MBBs in Figure 2, where only those three MBBs were able to stabilize the emulsions at pH 4.0 and no MBBs could produce emulsions at pH 10.0. Clearly, even if MBB-$B_{0.24}E_{0.76}$ and MBB-$B_{0.00}E_{1.00}$ at pH 4.0 and all PDEAEMA-containing MBBs at pH 10.0 decreased γ significantly, the individual bottlebrushes were not

strongly bound to the interface and were ejected from the interface when the interfacial area was reduced. Note that the lowering of γ reflects the adsorption of amphiphiles to the water-oil interface but does not necessarily correlate with emulsion stability, which has been reported in the literature.[10a,15b] The rheological properties of the adsorbed interfacial layer, related to the binding energy per emulsifier species to the interface, play an important role among many factors in determining if emulsion droplets are stable against coalescence.[15-18,20,31]

During the optical microscopy study of the emulsion droplets formed with 0.03 wt% MBB-$B_{0.51}E_{0.49}$ at pH 4.0, we serendipitously observed that, with solvent evaporation, emulsion droplets crumpled on themselves, leaving behind a wrinkled film (Figure 5E),[18,20,23-25] suggesting that the bottlebrushes formed a film at the interface. To further confirm these observations, we prepared an emulsion at pH 4.0 using 0.03 wt% MBB-$B_{0.51}E_{0.49}$ and transferred a small portion of the emulsion layer to a slide for observation under an optical microscope. As shown in Video-13 in the SI, with solvent evaporation, the interface wrinkled and the droplets crumpled. For the same MBB, although no stable emulsion could be generated at pH 10.0, we vortexed the mixture and examined the droplets quickly under the optical microscope; no wrinkling was observed when the solvents evaporated (Video-14 in the SI). We also used 0.03 wt% sodium dodecyl sulfonate to emulsify toluene and an acidic aqueous solution under the same conditions, which formed a toluene-in-water emulsion; the droplets shrank and then disappeared (Video-15 in the SI), and there was no interfacial wrinkling.

As mentioned earlier, this is the first observation of interfacial wrinkling from amphiphilic MBBs alone adsorbed at the oil-water interface. When the interfacial area was reduced, either by withdrawing of the pendant toluene droplet or through solvent evaporation, the strongly, irreversibly adsorbed bottlebrush molecules experienced an in-plane lateral compression at the interface. This compression could first cause the brushes to change their backbone conformation from extended to coiled to accommodate the reduced interfacial area per brush molecule before the interfacial layer undergoes wrinkling. As the first step toward the study of the conformational behavior of amphiphilic MBBs at the interface, we spread MBB-$B_{0.80}E_{0.20}$ onto the surface of a pH 4.0 aqueous solution in a Langmuir-Blodgett trough and compressed the monolayer to a surface pressure of 20 mN/m. AFM revealed that the brush backbone changed from extended to coiled conformations (Figure S23). Although this experiment does not directly correlate with the toluene-water interface, it shows the possibility of lateral compression-induced shape transitions of MBBs at the interface and the complexity of the interfacial behavior of amphiphilic MBBs. Further compression would force the brush layer

at the interface to wrinkle due to the strong, irreversible adsorption. The amplitude of the wrinkling pattern or the "apparent" thickness of the wrinkled layer depends on the degree of compression and the mechanical properties of the adsorbed layer, as revealed in other systems such as the interfacial layers assembled by electrostatic interactions.[20b] Under the extreme compression scenario, the wrinkled brush layer could be compressed to fold into a multilamellar interfacial layer (i.e., the film collapses), and it is possible that some MBBs with irregular structures (see Figure S23) are embedded in the collapsed interfacial layer.

Our results can be summarized by Figure 5F. At pH 4.0, PDEAEMA is protonated and only soluble in water, while PnBA is only soluble in toluene. Consequently, upon adsorption to the interface, the bottlebrushes with appropriate side chain compositions undergo spontaneous re-configuration into a Janus structure, with PnBA and charged PDEAEMA side chains extending only into the organic and the aqueous phase, respectively. Control experiments showed that a PDEAEMA homopolymer can be fully transferred from the top toluene layer into the bottom acidic aqueous phase in a vial under stirring conditions and the protonated PDEAEMA homopolymer in an acidic aqueous solution exhibited a negligible, unmeasurable partitioning coefficient to toluene. On the other hand, PnBA had no measurable solubility in water (see the details in the SI). The different attractions of PnBA and PDEAEMA for distinct liquid phases and the large molecular size of the MBBs impart a strong binding of MBBs to the interface and thus a high stability of emulsions. When the interfacial area is reduced, the high binding energy of the bottlebrushes prevents them from desorbing from the interface, resulting in possible shape changes and jamming of the brushes at the interface. When the pH is changed to 10.0, PDEAEMA is deprotonated and becomes insoluble in water, causing the brushes to desorb from the interface and the breaking of emulsions.

Conclusion

We showed that heterografted PnBA/PDEAEMA MBBs with appropriate side chain compositions were efficient and robust pH-responsive emulsifiers. The emulsions with an excellent long-term stability were formed at pH 4.0 and disrupted upon increasing the pH to 10.0. The formation and breaking of emulsions can be repeated $\geq$ 10 times by cycling the pH between 4.0 and 10.0 at concentrations $\geq$ 0.01 wt%, and the bottlebrushes remained intact. Pendant drop tensiometry showed that a decrease in γ was necessary but not sufficient for emulsion stabilization. When the interfacial area was reduced, jamming of bottlebrushes was only observed for the three MBBs that formed emulsions at pH 4.0, indicating the strong, irreversible adsorption of these

MBBs to the interface. This study demonstrates a method to design amphiphilic MBBs as efficient and effective stimuli-responsive emulsifiers by combining the particle-like properties from their large molecular sizes and the flexibility and responsiveness of block copolymers, opening new opportunities for potential applications of MBBs.

Acknowledgements

[1] a) M. Zhang,; A. H. E. Müller, *J. Polym. Sci. Part A: Polym. Chem.* **2005,** *43*, 3461-3481; b) S. S. Sheiko, B. S. Sumerlin, K. Matyjaszewski, *Prog. Polym. Sci.* **2008,** *33*, 759-785; c) Z. Li, M. Tang, S. Liang, M. Zhang, G. M. Biesold, Y. He, S.-M. Hao, W. Choi, Y. Liu, J. Peng, Z. Lin, *Prog. Polym. Sci.* **2021,** *116*, 101387; d) B. Zhao, *J. Phys. Chem. B* **2021**, *125*, 6373-6389; e) G. Xie, M. R. Martinez, M. Olszewski, S. S. Sheiko, K. Matyjaszewski, *Biomacromolecules* **2019,** *20*, 27-54; f) M. Müllner, *Chem. Commun.* **2022**, *58*, 5683-5716.

[2] a) S. S. Sheiko, S. A. Prokhorova, K. L. Beers, K. Matyjaszewski, I. I. Potemkin, A. R. Khokhlov, M. Möller, *Macromolecules* **2001,** *34*, 8354-8360; b) C. Li, N. Gunari, K. Fischer, A. Janshoff, M. Schmidt, *Angew. Chem. Int. Ed.* **2004,** *43*, 1101-1104; c) Y. Xu, S. Bolisetty, M. Ballauff, A. H. E. Müller, *J. Am. Chem. Soc.* **2009,** *131*, 1640-1641; d) H.-i. Lee, J. Pietrasik, S. S. Sheiko, K. Matyjaszewski, *Prog. Polym. Sci.* **2010,** *35*, 24-44; e) E. W. Kent, B. Zhao, *Macromolecules* **2019**, *52*, 6714-6724; f) H. Qi, X. Liu, D. M. Henn, S. Mei, M. C. Staub, B. Zhao, C. Y. Li, *Nature Commun.* **2020,** *11*, 2152.

[3] a) K. L. Beers, S. G. Gaynor, K. Matyjaszewski, S. S. Sheiko, M. Möller, *Macromolecules* **1998,** *31*, 9413-9415; b) G. Cheng, A. Böker, M. Zhang, G. Krausch, A. H. E. Müller, *Macromolecules* **2001,** *34*, 6883-6888; c) C. Cheng, K. Qi, E. Khoshdel, K. L. Wooley, *J. Am. Chem. Soc.* **2006,** *128*, 6808–6809; d) M. B. Runge, N. B. Bowden, *J. Am. Chem. Soc.* **2007,** *129*, 10551–10560; e) S. C. Radzinski, J. C. Foster, J. B. Matson, *Polym. Chem.***2015**, *6*, 5643–5652; f) M.-Q. Wang, H. Zou, W.-B. Liu, N. Liu, Z.-Q. Wu, *ACS Macro Letters* **2022,** *11*, 179-185.

[4] a) D. M. Henn, W. Fu, S. Mei, C. Y. Li, B. Zhao, *Macromolecules* **2017,** *50*, 1645-1656; b) D. M. Henn, C. M. Lau, C. Y. Li, B. Zhao, *Polym. Chem.* **2017**, *8*, 2702-2712; c) D. M. Henn, J. A. Holmes, E. W. Kent, B. Zhao, *J. Phys. Chem. B* **2018**, *122*, 7015-7025; d) A. E. Levi, J. Lequieu, J. D. Horne, M. W. Bates, J. M. Ren, K. T. Delaney, G. H. Fredrickson, C. M. Bates, *Macromolecules* **2019**, *52*, 1794–1802; e) X. Zhu, J. Zhang, C. Miao, S. Li, Y. Zhao, *Polym. Chem.* **2020**, *11*, 3003–3017; f) Y. Yan, C. Gao, J. Li, T. Zhang, G. Yang, Z. Wang, Z. Hua, *Biomacromolecules* **2020**, *21*, 613– 620; g) E. W. Kent, E. M. Lewoczko, B. Zhao, *Polym. Chem.* **2021**, *12*, 265-276; h) E. M. Lewoczko, M. T. Kelly, E. W. Kent, B. Zhao, *Soft Matter* **2021**, *17*, 6566-6579; i) T. Pan, S. Dutta, Y. Kamble, B. B. Patel, M. A. Wade, S. A. Rogers, Y. Diao, D. Guironnet, C. E. Sing, *Chem. Mater.* **2022**, *34*, 1990−2024; j) S. Li, P. Liu, Z. Wang, L. Lian, Y. Zhao, *Polym. Chem.* **2022**, *13*, 877-890.

[5] a) J. A. Johnson, Y. Y. Lu, A. O. Burts, Y. Xia, A. C. Durrell, D. A. Tirrell, R. H. Grubbs, *Macromolecules* **2010**, *43*, 10326-10335; b) J. Rzayev, *ACS Macro Letters* **2012,** *1*, 1146-1149; c) X. Banquy, J. Burdyńska, D. W. Lee, K. Matyjaszewski, J. Israelachvili, *J. Am. Chem. Soc.* **2014,** *136*, 6199-6202; d) A. L. Liberman-Martin, C. K. Chu, R. H. Grubbs, *Macromol. Rapid Commun.* **2017,** *38*, 1700058; e) H. Luo, M. Szymusiak, E. A. Garcia, L. L. Lock, H. Cui, Y. Liu, M. Herrera-Alonso, *Macromolecules* **2017,** *50*, 2201-2206; f) W. F. M. Daniel, G. Xie, M. Vatankhah Varnoosfaderani, J. Burdyńska, Q. Li, D. Nykypanchuk, O. Gang, K. Matyjaszewski, S. S. Sheiko, *Macromolecules* **2017,** *50*, 2103-2111; g) A. Detappe, H. V. T. Nguyen, Y. Jiang, M. P. Agius, W. Wang, C. Mathieu, N. K. Su, S. L. Kristufek, D. J. Lundberg, S. Bhagchandani, I. M. Ghobrial, P. P. Ghoroghchian, J. A. Johnson, *Nature Nanotech.* **2023**, *18*, 184-192; h) Y. Zhang, L. Fu, M. R. Martinez, H. Sun, V. Nava, J. Yan, K. Ristroph, S. E. Averick, B. Marelli, J. P. Giraldo, K. Matyjaszewski, R., R. D. Tilton, G. V. Lowry, *ACS Sustain. Chem. Eng.* **2023**, *11*, 3346-3358.

[6] a) D. Fournier, R. Hoogenboom, U. S. Schubert, *Chem. Soc. Rev.* **2007**, *36*, 1369-1380; b) H. Gao, K. Matyjaszewski, *J. Am. Chem. Soc.* **2007**, *129*, 6633-6639; c) A. C. Engler, H.-i. Lee, P. T. Hammond, *Angew. Chem. Int. Ed.* **2009**, *48*, 9334-9338; d) Y. Yan, Y. Shi, W. Zhu, Y. Chen, *Polymer* **2013**, *54*, 5634-5642; e) H. Tang, Y. Li, S. H. Lahasky, S. S. Sheiko, D. Zhang, *Macromolecules* **2011**, *44*, 1491–1499; f) D. Han, X. Tong, Y. Zhao, *Macromolecules* **2011**, *44*, 5531–5536; g) E. W. Kent, D. M. Henn, B. Zhao, *Polym. Chem.* **2018**, *9*, 5133-5144; h) E. W. Kent, E. M. Lewoczko, B. Zhao, *Langmuir* **2020**, *36*, 13320-13330.

[7] a) J. Israelachvili, *Colloids Surf. A* **1994**, *91*, 1–8; b) M. J. Lawrence, G. D. Rees, *Adv. Drug Delivery Rev.* **2000**, *45*, 89–121; c) A. Gupta, H. B. Eral, T. A. Hattona, P. S. Doyle, *Soft Matter* **2016**, *12*, 2826–2841.

[8] M. Hu, T. P. Russell, *Mater. Chem. Front.* **2021**, *5*, 1205-1220.

[9] a) Y. Li, J. Zou, B. P. Das, M. Tsianou, C. Cheng, *Macromolecules* **2012**, *45*, 4623-4629; b) Y. K. Li, L. Christian-Tabak, V. L. F. Fuan, J. Zou, C. Cheng, *J. Polym. Sci., Part A: Polym. Chem.* **2014**, *52*, 3250–3259.

[10] a) G. Xie, P. Krys, R. D. Tilton, K. Matyjaszewski, *Macromolecules* **2017,** *50*, 2942-2950; b) T. L. Hsieh, M. R. Martinez, S. Garoff, K. Matyjaszewski, R. D. Tilton, *J. Colloid Interface Sci.* **2020**, *581*, 135–147.

[11] H. Li, H. Miao, Y. Gao, H. M. Li, D. Y. Chen, *Polym. Chem.* **2016**, *7*, 4476–4485.

[12] F. Jia, F. Liang, Z. Yang, *Langmuir* **2018**, *34*, 1718–1724.

[13] Y. Gao, X. Wu, Z. Xiang, C. Qi, *Langmuir* **2021,** *37*, 2376-2385.

[14] a) X. Chen, X. Yang, D.-P. Song, Y.-F. Men, Y. Li, *Macromolecules* **2021,** *54* (8), 3668-3677; b) T. Yuan, Y. Li, D.-P. Song, *Macromol. Rapid Commun.* **2022**, *43*, 2200188

[15] a) H.-G. Seong, Z. Chen, T. Emrick, T. P. Russell, *Angew. Chem. Int. Ed.* **2022,** *61*, e202200530; b) Z. Chen, M. Hu, X. Li, D. M. Smith, H.-G. Seong, T. Emrick, J. Rzayev, T. P. Russell, *Angew. Chem. Int. Ed.* **2022**, *61*, e202201392.

[16] B. P. Binks, *Langmuir* **2017**, *33*, 6947–6963.

[17]   a) B. P. Binks, *Curr. Opin. Colloid Interface Sci.* **2002**, *7*, 21–41; b) R. Aveyard, B. P. Binks, J. H. Clint, *Adv. Colloid Interface Sci.* **2003**, *100–102*, 503–546;

[18]   a) M. Cui, T. Emrick, T. P. Russell, *Science* **2013**, *342*, 460–463; b) S. Shi, T. P. Russell, *Adv. Mater.* **2018**, *30*, 1800714; c) B. Wang, B. Yin, Z. Zhang, Y. Yin, Y. Yang, H. Wang, T. P. Russell, S. Shi, *Angew Chem. Int. Ed.* **2022**, *61*, e202114936.

[19]   a) T. M. Ruhland, A. H. Gröschel, A. Walther, A. H. Müller, *Langmuir* **2011**, *27*, 9807–9814; b) F. Tu, D. Lee, *J. Am. Chem. Soc.* **2014**, *136*, 9999−10006.

[20]   a) B. Wang, T. Liu, H. Chen, B. Yin, Z. Zhang, T. P. Russell, S. Shi, *Angew. Chem. Int. Ed.* **2021,** *60*, 19626-19630; b) H.-G. Seong, Z. Fink, Z. Chen, T. Emrick, T. P. Russell, *ACS Nano* **2023**, *17*, 14731–14741.

[21]   J. Tang, P. J. Quinlan, K. C. Tam, *Soft Matter* **2015,** *11*, 3512-3529.

[22]   J. Tang, R. M. Berry, K. C. Tam, *Biomacromolecules* **2016**, *17*, 1748-1756.

[23]   K. Liu, J. Jiang, Z. Cui, B. P. Binks, *Langmuir* **2017,** *33*, 2296-2305.

[24]   Z. Xia, C.-G. Lin, Y. Yang, Y. Wang, Z. Wu, Y.-F. Song, T. P. Russell, S. Shi, *Angew. Chem. Int. Ed.* **2022**, *61*, e202203741.

[25]   Y. Yang, H. Sun, M. Wang, M. Li, Z. Zhang, T. P. Russell, S. Shi, *Angew Chem. Int. Ed.* **2023**, *62*, e202218440.

[26]   N. Deirram, C. Zhang, S. S. Kermaniyan, A. P. R. Johnston, G. K. Such, *Macromol. Rapid Commun.* **2019,** *40*, 1800917.

[27]   A. A. Umar, I. B. M. Saaid, A. A. Sulaimon, R. B. M. Pilus, *J. Petrol. Sci. Eng.* **2018,** *165*, 673-690.

[28]   K. Zhou, Y. Wang, X. Huang, K. Luby-Phelps, B. D. Sumer, J. Gao, *Angew. Chem., Int. Ed.* **2011**, *50*, 6109– 6114,

[29]   a) D. M. Henn, R. A. E. Wright, J. W. Woodcock, B. Hu, B. Zhao, *Langmuir* **2014**, *30*, 2541–2550; b) M. T. Kelly, E. W. Kent, B. Zhao, *Macromolecules* **2022**, *55*, 1629-1641.

[30]   S. S. Datta, H. C. Shum, D. A. Weitz, *Langmuir* **2010,** *26*, 18612-18616.

[31]   F. Ravera, K. Dziza, E. Santini, L. Cristofolini, L. Liggieri, *Adv. Colloid Interace Sci.* **2021**, *288*, 102344.

11

Entry for the Table of Contents
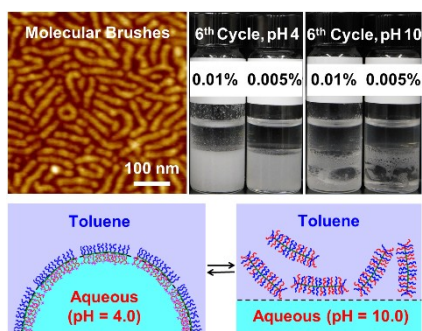
Molecular bottlebrushes with randomly grafted hydrophobic and pH-responsive polymer side chains are efficient and robust responsive emulsifiers for generation of water-in-oil emulsions, which exhibit both high stability, derived from large molecular sizes and interfacial Janus structures, and stimuli-responsive behavior. The formation and disruption of emulsions were repeated 10 times, and the bottlebrushes remained intact.